



## Heterogeneous Ozonolysis of Squalene: Gas-Phase Products Depend on Water Vapor Concentration

Arata, Caleb; Heine, Nadja; Wang, Nijing; Misztal, Pawel K.; Wargocki, Pawel; Bekö, Gabriel; Williams, Jonathan; Nazaroff, William W; Wilson, Kevin R.; Goldstein, Allen H.

*Published in:*  
Environmental Science and Technology

*Link to article, DOI:*  
[10.1021/acs.est.9b05957](https://doi.org/10.1021/acs.est.9b05957)

*Publication date:*  
2019

*Document Version*  
Peer reviewed version

[Link back to DTU Orbit](#)

### *Citation (APA):*

Arata, C., Heine, N., Wang, N., Misztal, P. K., Wargocki, P., Bekö, G., Williams, J., Nazaroff, W. W., Wilson, K. R., & Goldstein, A. H. (2019). Heterogeneous Ozonolysis of Squalene: Gas-Phase Products Depend on Water Vapor Concentration. *Environmental Science and Technology*, 53(24), 14441-14448. <https://doi.org/10.1021/acs.est.9b05957>

---

### General rights

Copyright and moral rights for the publications made accessible in the public portal are retained by the authors and/or other copyright owners and it is a condition of accessing publications that users recognise and abide by the legal requirements associated with these rights.

- Users may download and print one copy of any publication from the public portal for the purpose of private study or research.
- You may not further distribute the material or use it for any profit-making activity or commercial gain
- You may freely distribute the URL identifying the publication in the public portal

If you believe that this document breaches copyright please contact us providing details, and we will remove access to the work immediately and investigate your claim.

## Heterogeneous Ozonolysis of Squalene: Gas-Phase Products Depend on Water Vapor Concentration

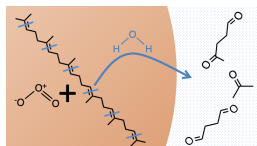
Caleb Arata, Nadja Heine, Nijing Wang, Pawel K. Misztal, Pawel Wargocki, Gabriel Beko, Jonathan Williams, William W. Nazaroff, Kevin R. Wilson, and Allen H. Goldstein

*Environ. Sci. Technol.*, **Just Accepted Manuscript** • DOI: 10.1021/acs.est.9b05957 • Publication Date (Web): 22 Nov 2019

Downloaded from [pubs.acs.org](https://pubs.acs.org) on November 25, 2019

### Just Accepted

“Just Accepted” manuscripts have been peer-reviewed and accepted for publication. They are posted online prior to technical editing, formatting for publication and author proofing. The American Chemical Society provides “Just Accepted” as a service to the research community to expedite the dissemination of scientific material as soon as possible after acceptance. “Just Accepted” manuscripts appear in full in PDF format accompanied by an HTML abstract. “Just Accepted” manuscripts have been fully peer reviewed, but should not be considered the official version of record. They are citable by the Digital Object Identifier (DOI®). “Just Accepted” is an optional service offered to authors. Therefore, the “Just Accepted” Web site may not include all articles that will be published in the journal. After a manuscript is technically edited and formatted, it will be removed from the “Just Accepted” Web site and published as an ASAP article. Note that technical editing may introduce minor changes to the manuscript text and/or graphics which could affect content, and all legal disclaimers and ethical guidelines that apply to the journal pertain. ACS cannot be held responsible for errors or consequences arising from the use of information contained in these “Just Accepted” manuscripts.



# Heterogeneous Ozonolysis of Squalene: Gas-Phase Products

## Depend on Water Vapor Concentration

Caleb Arata<sup>\*†§</sup>, Nadja Heine<sup>‡</sup>, Nijing Wang<sup>¶</sup>, Pawel K. Misztal<sup>§#</sup>, Pawel Wargocki<sup>^</sup>,  
Gabriel Bekö<sup>^</sup>, Jonathan Williams<sup>¶</sup>, William W Nazaroff<sup>¶</sup>, Kevin R. Wilson<sup>‡</sup>, Allen H.  
Goldstein<sup>§¶</sup>

<sup>†</sup>Department of Chemistry, <sup>§</sup>Department of Environmental Science, Policy and  
Management, and <sup>¶</sup>Department of Civil and Environmental Engineering, University of  
California, Berkeley, California 94720 United States

<sup>‡</sup>Chemical Sciences Division, Lawrence Berkeley National Laboratory, Berkeley, California  
94720, United States

<sup>¶</sup>Air Chemistry Department, Max Planck Institute for Chemistry, 55128 Mainz, Germany

<sup>^</sup>Department of Civil Engineering, Technical University of Denmark, 2800 Kgs. Lyngby,  
Denmark

<sup>#</sup>Now at: Department of Civil, Architectural and Environmental Engineering, The University of  
Texas at Austin, Austin, TX 78712

\*Phone: 310 968 8331. Email: caleb.arata@berkeley.edu

**Abstract**

19 Previous work examining the condensed-phase products of squalene particle ozonolysis found  
20 that an increase in water vapor concentration led to lower concentrations of secondary ozonides,  
21 increased concentrations of carbonyls, and smaller particle diameter, suggesting that water  
22 changes the fate of the Criegee intermediate. To determine if this volume loss corresponds to an  
23 increase in gas-phase products, we measured gas-phase volatile organic compound (VOC)  
24 concentrations via proton-transfer-reaction time-of-flight mass spectrometry. Studies were  
25 conducted in a flow-tube reactor at atmospherically relevant ozone ( $O_3$ ) exposure levels (5-30  
26 ppb h) with pure squalene particles. An increase in water vapor concentration led to strong  
27 enhancement of gas-phase oxidation products at all tested  $O_3$  exposures. An increase in water  
28 vapor from near zero to 70% relative humidity (RH) at high  $O_3$  exposure increased the total mass  
29 concentration of gas-phase VOCs by a factor of three. The observed fraction of carbon in the  
30 gas-phase correlates with the fraction of particle volume lost. Experiments involving  $O_3$   
31 oxidation of shirts soiled with skin oil confirms that the RH dependence of gas-phase reaction  
32 product generation occurs similarly on surfaces containing skin oil under realistic conditions.  
33 Similar behavior is expected for  $O_3$  reactions with other surface-bound organics containing  
34 unsaturated carbon bonds.

## 35 **Introduction**

36 People spend 90% of their lives indoors<sup>1</sup>. Each day, adult humans inhale 12-15 kg of air,  
37 making indoor air an important route of exposure to many chemicals, including volatile organic  
38 compounds (VOCs). People can be the dominant indoor VOC emission source in densely  
39 occupied spaces, and, in the presence of ozone (O<sub>3</sub>), the oxidation of skin lipids adds ketones and  
40 aldehydes to the composition of indoor air<sup>2-8</sup>.

41 Indoor O<sub>3</sub> concentrations are commonly 20-70% of outdoor levels, with the ratio  
42 depending on building air-change rate (ACR), type of ventilation system, and the nature of  
43 indoor surfaces<sup>9</sup>. Indoor air is estimated to contribute 25-60% of an individual's daily O<sub>3</sub>  
44 exposure.<sup>10</sup> In densely occupied spaces, occupants may be the dominant indoor sinks for O<sub>3</sub>,  
45 mainly due to reactions with lipids on their skin, hair, and clothing.<sup>11</sup>

46 Squalene (C<sub>30</sub>H<sub>50</sub>) constitutes 10% of the mass of human skin lipids, and contributes 50%  
47 of the unsaturated carbon bonds.<sup>12</sup> When exposed to O<sub>3</sub>, squalene is quickly oxidized to products  
48 that span a wide range of volatility; some products remain in the condensed phase while others  
49 become gaseous.<sup>5</sup>

50 Researchers have investigated effects of human occupancy on aircraft cabin air,  
51 considering that interior O<sub>3</sub> levels are sometimes elevated in airplanes.<sup>13</sup> Weschler et al.  
52 conducted experiments in a simulated aircraft cabin section and found that more than half of the  
53 observed oxidation products in the gas phase came from O<sub>3</sub> reacting with human skin lipids.<sup>4</sup>

54 Further work studied O<sub>3</sub> deposition on materials common to aircraft cabin interiors, finding that  
55 soiled clothing exposed to O<sub>3</sub> emits 6-methyl-5-hepten-2-one (6-MHO).<sup>14,15</sup> Surface bound  
56 squalene was found to have a high reaction probability with O<sub>3</sub>, in the range of  $0.5-1 \times 10^{-3}$ , and  
57 reaction of ozone with squalene on soiled clothing has been shown to be mass-transport  
58 limited.<sup>16-18</sup> Both 4-oxopentanal (4-OPA) and 6-MHO are known respiratory irritants.<sup>19,20</sup>  
59 Acetone and 6-MHO are among the most prominent VOCs emitted from human skin.<sup>21</sup> While  
60 acetone is known to originate from a wide variety of sources, including breath, 6-MHO is  
61 thought to be specific to squalene oxidation. The high emission rate suggests that squalene  
62 oxidation contributes significantly to VOC emissions from human skin.

63 Heine et al. investigated the influence of RH on squalene ozonolysis using pure squalene  
64 particles in a flow-tube reactor.<sup>22</sup> They showed that water vapor concentration does not affect the  
65 rate of squalene ozonolysis, but does substantially change the product composition. Under dry  
66 conditions, as O<sub>3</sub> consumes squalene, secondary ozonide concentrations increase in the  
67 condensed phase and initial particle volume is reduced by 15%. At 60% RH, condensed-phase  
68 ozonolysis products shift from secondary ozonides to carbonyls, and particle volume is reduced  
69 by as much as 50%. Such losses of particle volume should correspond to an increase in gas-  
70 phase oxidation products.

71 For this study, we designed experiments specifically to observe the mass lost to the gas

72 phase and the products formed by O<sub>3</sub>-squalene reactions as a function of RH, and to understand  
73 the implications for the fate of the Criegee intermediate on squalene particle surfaces and skin-oil  
74 coated clothing. Here, we investigate the gas-phase products from squalene particle ozonolysis in  
75 a flow tube reactor, and on skin-oil soiled shirts in a climate chamber. From the flow-tube  
76 experiments, we show that the RH dependent loss of particle diameter corresponds to an increase  
77 in gas-phase reaction products, consistent with the mechanism of water molecules promoting  
78 carbonyl formation from the Criegee intermediate under real world conditions. We discuss  
79 implications for product yields from skin oil ozonolysis indoors under varying RH conditions.

## 80 **Experimental Methods**

81 Squalene ozonolysis was carried out in a flow-tube reactor, as described in Heine et al.<sup>22,23</sup>  
82 Liquid squalene in a tube furnace was heated to 145 °C, generating, by means of homogeneous  
83 nucleation, polydisperse particles with a mean surface-weighted diameter of 250 +/- 40 nm. A  
84 continuous flow of 300 standard cm<sup>3</sup> min<sup>-1</sup> dry nitrogen (N<sub>2</sub>) carried the particles from the  
85 furnace through a charcoal denuder to remove any gas-phase contamination. This flow was then  
86 combined with flows of oxygen (O<sub>2</sub>), O<sub>3</sub>, dry N<sub>2</sub>, and humidified N<sub>2</sub> for a total flow of 1 L min<sup>-1</sup>.  
87 Levels of O<sub>2</sub> were held at a constant 10%, while the flows of dry and humidified N<sub>2</sub> were varied  
88 to give a range of nearly 0% (< 3%) to 100% RH. This combined flow traversed the flow tube



89 reactor (130 cm long, 2.5 cm inner diameter) with a residence time of 37 s.<sup>24</sup> Ozone was  
90 produced by a corona discharge generator, and the concentrations of O<sub>3</sub> were in the range 0-4  
91 ppm, giving O<sub>3</sub> exposures of 0-44 ppb h. The initial particle loading in the flow reactor was 1000  
92 μg m<sup>-3</sup>.

93       Upon leaving the flow-tube reactor, the outflow composition was measured by proton-  
94 transfer-reaction time-of-flight mass spectrometry (Ionicon PTR-TOF-MS 8000), an electrostatic  
95 classifier (TSI model 3080L) with a butanol-based condensation particle counter (TSI model  
96 3772), and a custom-built vacuum ultraviolet aerosol mass spectrometer (VUV-AMS). The  
97 particle size and composition measurements are described in Heine et al.<sup>22</sup>; the PTR-TOF-MS  
98 was used to measure speciated gas-phase VOC concentrations.

99       PTR-TOF-MS is a chemical ionization technique with minimal fragmentation using H<sub>3</sub>O<sup>+</sup>  
100 as the primary reagent ion. PTR-TOF-MS has been previously used to detect gas-phase products  
101 of squalene ozonolysis.<sup>2,4,5</sup> For these experiments, the instrument was calibrated with a  
102 multicomponent VOC gas standard to ensure stability throughout the campaign. Of the  
103 compounds reported here, only acetone was determined using a direct calibration. All other  
104 compound concentrations were calculated using a default proton transfer reaction rate constant of  
105  $2.5 \times 10^{-9} \text{ cm}^3 \text{ s}^{-1}$  for both the primary ion, H<sub>3</sub>O<sup>+</sup>, as well as for the first water cluster,  
106 H<sub>3</sub>O<sup>+</sup>(H<sub>2</sub>O). Direct calibration accuracies are estimated to be +/- 10%, whereas concentration

107 accuracies derived from the default rate constant are typically +/- 50%.<sup>25</sup> Increases in RH can  
108 cause increases in instrument sensitivities for certain compounds. However, these changes are  
109 typically a few percent, much lower than concentration differences reported in this work.<sup>26,27</sup>

110 Measurements of VOCs at each specified RH and O<sub>3</sub> exposure were made by allowing  
111 concentrations in the reactor to stabilize. Once stable, the particle flow was quickly replaced with  
112 a flow of N<sub>2</sub>. After 2 min, 95% of the particles were removed from the reactor, and a background  
113 concentration was taken. To account for both compounds being desorbed from the flow-tube  
114 walls as well as compounds being produced by heterogeneous oxidation on the walls, O<sub>3</sub> flow  
115 was maintained during the background sampling procedure. The difference between the stable  
116 concentration and the background concentration was taken to be the gas-phase concentration  
117 attributable to squalene-particle ozonolysis. Tables S1–S5 show the concentrations for each  
118 species as measured from the flow tube, as well as the measured background.

119 An experiment to analyze emissions from skin-oil soiled clothing under varying  
120 conditions of RH and O<sub>3</sub> was performed as part of the Indoor Chemical Human Emissions and  
121 Reactivity (ICHEAR) project. Four identical T-shirts (100% cotton) were washed with  
122 fragrance-free detergent and tumble dried, before being worn by four people overnight  
123 (minimum of 8 h). The skin-oil soiled T-shirts were then placed inside a stainless-steel climate  
124 chamber (volume 26.8 m<sup>3</sup>) ventilated with an air-change rate of 3.2 h<sup>-1</sup>. Outdoor air was used for

125 ventilation. It was filtered using particle and activated carbon filters to avoid interference from  
126 outdoor VOCs, and conditioned to reach the required temperature and RH. Ozone was generated  
127 (Jelight Model 600 UV) in the HVAC system downstream of the activated carbon filter and  
128 continuously introduced into the chamber at levels between 95-100 ppb. The temperature inside  
129 the chamber was maintained at 27.4–28.3 °C during the experiment and the O<sub>3</sub> levels were  
130 monitored throughout. Four RH levels were established. The lowest RH levels (at the beginning  
131 and end of the experiment) were not controlled (humidifier off, no dehumidifying present), while  
132 the two higher RH levels were achieved by operating a steam humidifier in the HVAC system.  
133 The first three levels were maintained for 1.5-2 hours to allow steady-state conditions to be  
134 reached. The resulting average RH levels during these three periods were 26%, 41%, and 56%.  
135 The final, fourth, RH condition was a decay from 50% to 28% with the humidifier off. The  
136 average RH for this period was 33%.

137 A PTR-TOF-MS (8000, Ionicon Analytik GmbH Innsbruck, Austria) was deployed  
138 during ICHEAR to monitor VOCs produced from O<sub>3</sub> oxidation of skin oil. The operational  
139 conditions of the PTR-TOF-MS were drift tube pressure 2.2 mbar, temperature 60 °C and 137 Td  
140 (*E/N*). The 3.2-mm (1/8”) Teflon inlet of the instrument was attached to the main exhaust duct of  
141 the chamber, approximately 1 m from the terminal through which the air was exhausted from the  
142 chamber and set to draw 100 mL min<sup>-1</sup> (via a main high flow inlet of 7 L min<sup>-1</sup>) continuously

143 into the mass spectrometer. Data reported for the skin-oil T-shirt experiment represent sample  
144 time resolution of 20 s. Before putting T-shirts inside the chamber, a background level of the  
145 empty chamber was established and maintained for 10 minutes. The measured background VOC  
146 levels were subsequently subtracted from the VOC levels measured while the T-shirts were in  
147 the chamber.

## 148 **Results and Discussion**

149 Figure 1 shows the chemical structures of squalene and selected gas-phase ozonolysis  
150 products. The first-generation gas-phase products are acetone, 6-methyl-5-hepten-2-one (6-  
151 MHO), and geranylacetone. Terminal oxidation products found in the gas phase, i.e. products  
152 that are minimally reactive with O<sub>3</sub> because of their lack of carbon-carbon double bonds, are  
153 acetone, 4-oxopentanal (4-OPA), and 1,4-butanedial (succinaldehyde). Scheme 1 shows a  
154 simplified mechanism for alkenes reacting with O<sub>3</sub>. In **R1**, O<sub>3</sub> adds across the double bond,  
155 forming a primary ozonide (not shown), which quickly decomposes to one of two combinations  
156 of carbonyl and Criegee intermediate. This reaction is fast and does not include water, so water  
157 vapor concentration has no effect on the rate of alkene loss.<sup>22</sup> The Criegee intermediate produced  
158 by **R1** is reactive, and can proceed through **R2** or **R3**, as well as through rearrangement or  
159 reactions with carboxylic acids<sup>28,29</sup>. **R2** shows the Criegee intermediate reacting with water to

160 form the  $\alpha$ -hydroxyhydroperoxide, which decomposes to a carbonyl and to hydrogen peroxide.  
161 **R3** shows the Criegee intermediate reacting with another carbonyl to form a secondary ozonide.  
162 The carbonyl products are more volatile than their respective secondary ozonides; in the  
163 presence of water, **R2** occurs faster than **R3**, leading to greater release of reaction products to the  
164 gas phase and a concomitant shrinking of the particle.

165       Figures 2A and 2B show the gas-phase concentration of geranylacetone and 6-MHO  
166 exiting the flow-tube reactor as a function of O<sub>3</sub> exposure and RH. Both compounds are primary  
167 products of squalene oxidation, and both have carbon-carbon double bonds that can further react  
168 with O<sub>3</sub>. At all RH levels, geranylacetone production peaks at an O<sub>3</sub> exposure of 10 ppb h. Dry  
169 conditions yield 5  $\mu\text{g m}^{-3}$  of geranylacetone, whereas more humid conditions (70% RH) enhance  
170 the concentration to 19  $\mu\text{g m}^{-3}$ , an increase by almost 4 $\times$ . More humid conditions, specifically  
171 RH of 30% and 50%, also show an increase in geranylacetone concentration compared to dry  
172 conditions. At exposures of 20 ppb h, the geranylacetone is fully consumed by ozonolysis and is  
173 not detected. Compared to other products measured, concentrations of geranylacetone are small.  
174 As a 13-carbon ketone, with a vapor pressure of 3.5 Pa at 298 K, most of the geranylacetone is  
175 expected to remain in the condensed phase.<sup>6</sup> Furthermore, there are fewer possible reaction  
176 pathways to produce geranylacetone than the other, shorter chain products. The low  
177 concentration measured in this study is consistent with a classroom study by Tang et al., where

178 both 6-MHO and 4-OPA were found at significantly higher concentrations than geranylacetone.<sup>2</sup>

179       The production of 6-MHO shows strong RH dependence. At all levels of O<sub>3</sub> exposure, an  
180 increase in RH leads to an increase in 6-MHO concentration. As 6-MHO is a primary product  
181 that can also be consumed, peak concentrations are found at the lower levels of O<sub>3</sub> exposure. At  
182 70% RH and 12 ppb h of O<sub>3</sub> exposure, the detected concentration is 170 μg m<sup>-3</sup>, 3 times the level  
183 of 6-MHO detected at the same O<sub>3</sub> exposure but under dry conditions. Unlike geranylacetone, 6-  
184 MHO is detected at even the highest levels of O<sub>3</sub> exposure tested, 30 ppb h. The 6-MHO species  
185 is used as a primary tracer compound for squalene oxidation, along with 4-OPA as a secondary  
186 tracer. The fact that 6-MHO is consumed at higher O<sub>3</sub> exposures, while 4-OPA is not, suggests  
187 that 6-MHO concentrations could be used as a proxy indicator for the age of oxidation products:  
188 at longer timescales, 6-MHO becomes depleted while 4-OPA does not.

189       Figures 3A-3C show the gas-phase concentrations as a function of O<sub>3</sub> exposure and RH  
190 of the three terminal products: acetone, 4-OPA, and 1,4-butanediol. At most levels of O<sub>3</sub>  
191 exposure, increasing RH produces increasing concentrations of acetone, again showing strong  
192 humidity dependence. At very low O<sub>3</sub> exposure (5-6 ppb h), 30% RH produces 32 μg m<sup>-3</sup> of  
193 acetone, whereas 70% RH conditions give 77 μg m<sup>-3</sup>, an increase by more than 2×. Under dry  
194 conditions, acetone increases to 100 μg m<sup>-3</sup> at 12 ppb h exposure, and then does not increase with  
195 increasing O<sub>3</sub> exposure. As acetone does not have carbon-carbon double bonds, it does not react

196 significantly with O<sub>3</sub> and so increasing exposure is not expected to consume acetone. Under  
197 higher RH conditions, the same leveling off is seen, but at higher concentrations. At 70% RH,  
198 acetone concentrations begin to plateau at 20 ppb h exposure, at a concentration of 280 μg m<sup>-3</sup>.  
199 At O<sub>3</sub> exposures greater than 10 ppb h, increasing RH from 0% to 70% increases acetone  
200 concentrations by a factor of 2.5 to 3.

201 Figure 3B shows the RH dependence of 4-OPA from the ozonolysis of squalene. A  
202 minimum of two reactions involving O<sub>3</sub> are required to produce 4-OPA from squalene, so  
203 concentrations are observed to increase later than the primary products, acetone and 6-MHO.  
204 Despite being a terminal product, 4-OPA does not show the same leveling off behavior as  
205 acetone. Under dry conditions, production stops increasing at 20 ppb h O<sub>3</sub> exposure, but under  
206 high RH conditions no leveling off is seen; production of 4-OPA may increase past 30 ppb h  
207 exposure. At O<sub>3</sub> exposures less than 12 ppb h, no RH dependence is seen, but production is also  
208 small. At higher O<sub>3</sub> exposures, 4-OPA shows strong RH dependence, with a factor of 6 increase  
209 in concentration between dry and humid conditions at 30 ppb h O<sub>3</sub> exposure. In both mixing ratio  
210 and mass concentration, 4-OPA is the most abundant gas-phase product, with a peak  
211 concentration of 600 μg m<sup>-3</sup>. If each double bond in squalene proceeds through reaction **R2**, one  
212 molecule of squalene would produce a single 1,4-butanedial molecule, two acetone molecules,  
213 and four 4-OPA molecules. While the observed mixing ratios of terminal products do not follow

214 these stoichiometric ratios, the relatively large number of 4-OPA molecules that can be made  
215 from each squalene molecule help to explain why it is the most abundant gas-phase product.

216 Figure 3C shows the concentration of 1,4-butanedial as a function of RH and O<sub>3</sub>  
217 exposure. As a terminal product, abundance of this species increases with O<sub>3</sub> exposure, and, for  
218 some RH conditions, eventually levels off. As with 4-OPA, production of 1,4-butanedial requires  
219 a minimum of two ozonolysis reactions, so concentrations substantially increase at greater O<sub>3</sub>  
220 exposure. Production of 1,4-butanedial shows a more complicated relation to RH than other  
221 species. The lowest levels of production, across all O<sub>3</sub> exposures, are under the most humid  
222 conditions. The next lowest levels of production are under the driest conditions. Although it does  
223 not follow the pattern of the other species measured, 1,4-butanedial levels do show strong  
224 variability with RH. At 30 ppb h O<sub>3</sub> exposure, switching from 70% RH to 30% RH increases the  
225 concentration of 1,4-butanedial from 52 μg m<sup>-3</sup> to 140 μg m<sup>-3</sup>. This ~3× increase in production is  
226 in line with the 3-6× changes in production observed at different RH for other compounds. The  
227 fact that 1,4-butanedial production peaks at intermediate RH, and declines at low and high RH,  
228 suggests that water plays a more complicated role than depicted in Scheme 1. Specifically,  
229 reaction **R2** increases 1,4-butanedial production up to a point, and then facilitates other reactions  
230 that suppress production.

231 Wisthaler and Weschler (2010) observed 12 prominent VOCs from squalene ozonolysis,



232 including the five compounds already discussed.<sup>5</sup> When glass wool soiled with human skin oil  
233 was exposed to O<sub>3</sub> (0-75 ppb h), three species — 4-methyl-8-oxo-4-nonenal (4-MON), 4-methyl-  
234 4-octene-1,8-dial (4-MOD), and 1-hydroxy-6-methyl-5-hepten-2-one (OH-6MHO) — showed  
235 mixing ratios similar to the observed mixing ratios of 4-OPA and 1,4-butanediol. These species  
236 were also observed during ozonolysis of a pure squalene film; however, the mixing ratios for that  
237 experiment were not reported. In our work, all three compounds were detected (4-MON, 4-  
238 MOD, and OH-6MHO), but at very low concentrations, 2 μg m<sup>-3</sup> or less. Possibly due to the low  
239 concentration of these species, a RH dependence isn't discernible.

240 Four other compounds identified by Wisthaler and Weschler (2010) — 1-hydroxypropan-  
241 2-one (hydroxyacetone), 4-oxobutanoic acid, and the isobaric compounds 5-hydroxy-4-  
242 oxopentanal and 4-oxopentanoic acid (levulinic acid) — are found in the present work at peak  
243 concentrations much lower than 6-MHO, acetone, 4-OPA, and 1,4-butanediol (5-15 μg m<sup>-3</sup>  
244 versus 140-600 μg m<sup>-3</sup>). All four compounds are terminal products; concentrations either  
245 increase or level off with increasing O<sub>3</sub> exposure, and none of the products show increasing  
246 production with increasing RH. Hydroxyacetone shows a muted response to changes in RH, as  
247 seen in Figure S6. Production is similar at 30% RH, 50% RH, and 70% RH, but increase by ~50-  
248 100% under dry conditions. Concentrations are modest, peaking at 15 μg m<sup>-3</sup> under dry  
249 conditions and 30 ppb h O<sub>3</sub> exposure. Levulinic acid or 5-hydroxy-4-oxopentanal (or a

250 combination of the two) only shows a RH effect at the highest O<sub>3</sub> exposure. At 30 ppb h, 70%  
251 RH yields 7 μg m<sup>-3</sup> while 30% RH produces 15 μg m<sup>-3</sup>, as seen in Figure S7. Figure S8 shows 4-  
252 oxobutanoic acid production *decreasing* with increased RH. At 70% RH and 30 ppb h O<sub>3</sub>  
253 exposure, we observe 1 μg m<sup>-3</sup>, whereas under dry conditions we measure 5 μg m<sup>-3</sup>.

254 One fragmentation ion was produced in quantities comparable to those of the dominant  
255 products, *m/z* 43.018 Da, C<sub>2</sub>H<sub>3</sub>O<sup>+</sup>. This fragment is common to acetic acid and acetate esters, but  
256 ions consistent with these parent masses were only found in low concentrations, so it is  
257 unassigned.<sup>30</sup> The fragment was found at mixing ratios comparable to 1,4-butanediol, and shows  
258 similar responses to RH.

259 To explore whether our gas-phase measurements agree with the amount of material lost  
260 from the particle phase, we summed the amount of carbon detected in the gas-phase products at  
261 different levels of RH. We used a carbon-balance approach to test whether the loss of material  
262 from the particle phase could be accounted for by generation of gas-phase products. The  
263 concentration of squalene entering the flow tube reactor was 1000 μg m<sup>-3</sup>, corresponding to 880  
264 μg m<sup>-3</sup> of carbon. Converting the measurements in Figures 2-3 from μg m<sup>-3</sup> to μg C m<sup>-3</sup>, and  
265 normalizing to the initial concentration of carbon entering the flow tube, gives the percent carbon  
266 in the gas phase. (As with the reported concentrations, these measurements are accurate to +/-  
267 50% for all species except for acetone, which is accurate to +/- 10% because it is directly

268 calibrated.) Figure 4 shows the percent carbon in the gas phase at 20 ppb h O<sub>3</sub> exposure. Note  
269 that only the dominant products are shown. Switching from 0% RH to 70% RH increases the  
270 proportion of carbon entering the gas phase from 21% to 65%, with increases in all dominant  
271 products except 1,4-butanediol. Assuming that an average of two molecules of oxidation  
272 products are generated for each molecule of ozone that reacts with squalene, this outcome  
273 corresponds to yields of between 42% and 130% for gas-phase oxidation products per molecule  
274 of ozone consumed. Even a moderate change, from dry conditions to 30% RH, increases the  
275 proportion of carbon entering the gas phase by 60%. The largest increases are seen in 4-OPA  
276 production.

277       Because the VUV-AMS only measures relative concentrations of species, there is no  
278 direct measurement of the amount of carbon present in the condensed phase. However,  
279 measurements of the change in particle volume can be used as a quantitative indicator for mass  
280 loss from the particle. Note that this approach ignores any mass gained by the addition of oxygen  
281 to condensed phase products of ozonolysis, as well as any difference in densities between  
282 squalene and condensed-phase reaction products. Despite these limitations, using this approach,  
283 there is a clear and strong correlation between the carbon detected in the gas phase and the  
284 volume lost from the particle, as shown in Figure 5. Under dry conditions, at all levels of O<sub>3</sub>  
285 exposure, ~20% of the particle volume is lost, and ~20% of the carbon from squalene is found in

286 the gas phase. At higher RH values, both the particle volume lost and the amount of carbon  
287 entering the gas phase are more sensitive to O<sub>3</sub> exposure, as shown by the larger spread for these  
288 humidified conditions. The highest RH level (70%) gives both the greatest particle volume loss  
289 and the largest percent of carbon in the gas phase. Notwithstanding experimental uncertainties,  
290 the evidence displayed in Figure 5 is consistent with expectations for the quantitative loss of  
291 particle-phase carbon being balanced with increased abundances of gaseous carbon species.

292         Figures 6 and S9 show the measurements in chamber air of several pertinent VOCs along  
293 with O<sub>3</sub> and RH. Four T-shirts were placed inside the measurement chamber at 10:25 with RH  
294 maintained at ~26% for 1.5 h. Thereafter the RH was increased in a series of steps. The  
295 previously identified squalene oxidation products (4-OPA, 1,4-butanedial, acetone, 6-MHO, and  
296 geranylacetone) were observed to vary in response to the changing RH levels. Owing to the  
297 working principle of the humidifier, the RH in the chamber fluctuated regularly within a 10%  
298 range with a cycle of 38 minutes. In the data shown, primary unsaturated products and terminal  
299 products all faithfully follow the RH variation, confirming the dependence of gas-phase squalene  
300 ozonolysis products on RH, consistent with the flow-tube experiments. In accordance with  
301 previous studies, 4-OPA was the most abundant product (especially at higher RH levels);  
302 geranylacetone concentration was consistently the lowest among the quantified species.

303         In contrast with the flow-tube experiment, in which squalene particles were continuously

304 supplied, the skin-oil soiled T-shirts contained a limited amount of squalene that was  
305 progressively consumed by O<sub>3</sub>. Therefore, at any given RH, most of the compounds showed a  
306 decreasing trend as the available squalene was depleted, except the first level where the lagging  
307 terminal products still increase towards steady state. In particular, acetone clearly followed the  
308 RH modulation while steadily decreasing as the experiment progressed. To better quantify the  
309 relative yields of the VOCs as a function of RH, two pairs of RH levels were selected,  
310 corresponding to points labeled 1-4 in Figure 6. As shown in Table 1, the concentration of 4-  
311 OPA increased by 5.9 µg m<sup>-3</sup> as the RH increased from 26% (point 1) to 44% (point 2). A  
312 similar increase of 5.1 µg m<sup>-3</sup> was seen in a second cycle as the RH changed from 46% (point 3)  
313 to 59% (point 4). The other terminal products (1,4-butanedial, hydroxy acetone, 4-oxobutanoic  
314 acid and 5-hydroxy-4-oxopentanal/levulinic acid) also showed slightly higher yields during the  
315 first RH increase (point 1 to point 2). Although the level of the first-generation products  
316 (acetone, 6-MHO and geranylacetone) tended to decrease with time, an increase was still  
317 observed in the second step (points 3 and 4) when the RH increased from 46% to 59%. However,  
318 unlike 4-OPA, the concentration changes were much lower than during the first RH increase  
319 (points 1 and 2), as shown in Table 1. For 6-MHO and geranylacetone, additional oxidation by  
320 O<sub>3</sub> could also be a contributing factor. Ozone removal was 3.4 ppb in the second RH step (46%  
321 to 59%), compared to 2.9 ppb in the first step, indicating that more 6-MHO and geranylacetone

322 were produced and subsequently oxidized by O<sub>3</sub> at this stage. Significantly elevated 4-OPA  
323 concentrations after the second increase of RH further supports this explanation.

324         Effects of RH on squalene ozonolysis have been observed in prior studies. Petrick and  
325 Dubowski studied the condensed phase of squalene film oxidation while varying RH, finding  
326 that increased RH led to more ketone production.<sup>31</sup> They also note that RH did not influence  
327 reaction kinetics, a finding also reported by Fu et al.<sup>32</sup> Wang and Waring examined secondary  
328 organic aerosol formation from the ozonolysis of surface-film squalene at 21% RH and 51%  
329 RH.<sup>33</sup> At high O<sub>3</sub> exposures, they found that the higher RH increased the aerosol mass fraction  
330 (AMF) from squalene. This increase suggests that higher RH leads to more oxidation products  
331 entering the gas phase, where they then can condense onto airborne particles. Zhou et al.  
332 examined the RH dependence of squalene film oxidation on the condensed phase products,  
333 finding that increasing the RH increased the yield of lower molecular weight products and  
334 decreased the yield of higher molecular weight products.<sup>34</sup> Although not quantitatively  
335 comparable, these previous studies qualitatively agree that an increase in RH leads to an increase  
336 in volatile products from squalene ozonolysis.

337         Humidity is already known to be an important factor that can influence VOC emissions  
338 from materials, compete with VOCs for sorptive uptake, and influence how indoor air is  
339 perceived.<sup>35-44</sup> Humidity is also known to change the rate of uptake of O<sub>3</sub> on indoor surfaces, a

340 relationship that varies among common indoor materials.<sup>45</sup> Few studies have assessed how RH  
341 changes ozonolysis products and emission rates. Coleman et al. (2008) found that increasing RH  
342 from 10% to 50% doubled the emissions of most ozonolysis byproducts from a cotton surface,  
343 with nonanal and decanal emissions increasing by about 5 $\times$ .<sup>14</sup> Gall et al. (2013) studied primary  
344 and secondary ozonolysis emissions from building materials, finding RH to have mixed effects.<sup>46</sup>  
345 Secondary emissions increased with RH for painted drywall, while emissions from carpet and  
346 ceiling tile did not. The present work contributes new knowledge, showing that RH can directly  
347 influence the products of squalene ozonolysis, providing an alternate route by which water vapor  
348 can increase VOC concentrations. At realistic indoor O<sub>3</sub> exposures, a change from 0% RH to  
349 70% RH results in  $\sim$ 3 times the amount of carbon entering the gas phase. Squalene, with six  
350 carbon-carbon double bonds, is a model molecule to show this effect. Other unsaturated  
351 compounds, especially those with double bonds separating small moieties, may show similar  
352 behavior. The reactions shown in Scheme 1 are not specific to squalene, and so long as the  
353 carbonyls formed by reaction **R2** have sufficient volatility, increased production of gas-phase  
354 products are generally expected from increases in RH.

355         The effects seen in this study suggest that RH can significantly alter the gas-phase  
356 composition of indoor air. In high occupancy settings, skin-oil oxidation can be the dominant  
357 source of VOCs, and changes in RH can alter the strength of this source by as much as a factor

358 of 3.<sup>4</sup> In the flow-tube reactor, at the highest level of O<sub>3</sub> exposure and RH, the sum of the  
359 concentrations of dominant products was 940 μg m<sup>-3</sup>, comparable to the 1000 μg m<sup>-3</sup> of squalene  
360 entering the reactor. It should be noted that RH does not change the rate of squalene ozonolysis:  
361 at low RH, oxidized products are still being formed, but remain in the condensed phase. If that  
362 condensed phase is the skin surface, then the products might be taken up dermally, where they  
363 might influence health.<sup>19,47</sup> The large effect of RH on ozonolysis products from squalene, and the  
364 potential for the underlying mechanism to act on other alkenes, warrants further research on how  
365 humidity may modulate indoor reactive chemistry and its consequences.

366

367 **Supporting Information.** Tables of raw and background concentrations of species measured for  
368 this study. Figures for species not seen in large quantities.

369 **Acknowledgments.** The UC Berkeley team was funded by the Alfred P. Sloan Foundation via  
370 Grant 2016-7050. Kevin R. Wilson and Nadja Heine were supported by the Department of  
371 Energy, Office of Science, Office of Basic Energy Sciences, Chemical Sciences, Geosciences,  
372 and Biosciences Division, in the Gas Phase Chemical Physics Program under Contract No. DE-  
373 AC02-05CH11231. This research used resources of the Advanced Light Source, which is a DOE  
374 Office of Science User Facility under contract no. DE-AC02-05CH11231. The ICHEAR team  
375 (MPI and DTU) were funded by the Alfred P. Sloan Foundation via Grant G-2018-11233. Allen



376 H. Goldstein gratefully acknowledges a Humboldt Research Award from the Alexander von  
377 Humboldt Foundation. The authors gratefully acknowledge members of the ICHEAR team  
378 including Nora Zannoni, Mengze Li, and Lisa Ernle for their contributions in performing the T-  
379 shirt experiments.

## 380 **References**

- 381 (1) Klepeis, N. E.; Nelson, W. C.; Ott, W. R.; Robinson, J. P.; Tsang, A. M.; Switzer, P.;  
382 Behar, J. V.; Hern, S. C.; Engelmann, W. H. The National Human Activity Pattern Survey  
383 (NHAPS): A Resource for Assessing Exposure to Environmental Pollutants. *J. Exposure*  
384 *Anal. Environ. Epidemiol.* **2001**, *11*, 231–252.
- 385 (2) Tang, X.; Misztal, P. K.; Nazaroff, W. W.; Goldstein, A. H. Volatile Organic Compound  
386 Emissions from Humans Indoors. *Environ. Sci. Technol.* **2016**, *50*, 12686–12694.
- 387 (3) Weschler, C. J. Roles of the human occupant in indoor chemistry. *Indoor Air* **2016**, *26*, 6–  
388 24.
- 389 (4) Weschler, C. J.; Wisthaler, A.; Cowlin, S.; Tamás, G.; Strøm-Tejsten, P.; Hodgson, A. T.;  
390 Destailats, H.; Herrington, J.; Zhang, J.; Nazaroff, W. W. Ozone-Initiated Chemistry in  
391 an Occupied Simulated Aircraft Cabin. *Environ. Sci. Technol.* **2007**, *41*, 6177–6184.
- 392 (5) Wisthaler, A.; Weschler, C. J. Reactions of ozone with human skin lipids: Sources of  
393 carbonyls, dicarbonyls, and hydroxycarbonyls in indoor air. *Proc. Natl. Acad. Sci.* **2010**,  
394 *107*, 6568–6575.
- 395 (6) Lakey, P. S. J.; Wisthaler, A.; Berkemeier, T.; Mikoviny, T.; Pöschl, U.; Shiraiwa, M.  
396 Chemical kinetics of multiphase reactions between ozone and human skin lipids:

- 397 implications for indoor air quality and health effects. *Indoor Air* **2017**, *27*, 816–828.
- 398 (7) Lakey, P. S. J.; Morrison, G. C.; Won, Y.; Parry, K. M.; von Domaros, M.; Tobias, D. J.;  
399 Rim, D.; Shiraiwa, M. The impact of clothing on ozone and squalene ozonolysis products  
400 in indoor environments. *Commun. Chem.* **2019**, *2*, 56.
- 401 (8) Kruza, M.; Carslaw, N. How do breath and skin emissions impact indoor air chemistry?  
402 *Indoor Air* **2019**, *29*, 369–379.
- 403 (9) Weschler, C. J. Ozone in indoor environments: Concentration and chemistry. *Indoor Air*  
404 **2000**, *10*, 269–288.
- 405 (10) Weschler, C. J. Ozone's Impact on Public Health: Contributions from Indoor Exposures to  
406 Ozone and Products of Ozone-Initiated Chemistry. *Environ. Health Perspect.* **2006**, *114*,  
407 1489–1496.
- 408 (11) Fischer, A.; Ljungström, E.; Langer, S. Ozone removal by occupants in a classroom.  
409 *Atmos. Environ.* **2013**, *81*, 11–17.
- 410 (12) Nicolaides, N. Skin Lipids: Their Biochemical Uniqueness. *Science.* **1974**, *186*, 19–26.
- 411 (13) Bhangar, S.; Cowlin, S. C.; Singer, B. C.; Sextro, R. G.; Nazaroff, W. W. Ozone Levels in  
412 Passenger Cabins of Commercial Aircraft on North American and Transoceanic Routes.  
413 *Environ. Sci. Technol.* **2008**, *42*, 3938–3943.
- 414 (14) Coleman, B. K.; Destailats, H.; Hodgson, A. T.; Nazaroff, W. W. Ozone consumption  
415 and volatile byproduct formation from surface reactions with aircraft cabin materials and  
416 clothing fabrics. *Atmos. Environ.* **2008**, *42*, 642–654.
- 417 (15) Wisthaler, A.; Tamás, G.; Wyon, D. P.; Strøm-Tejsen, P.; Space, D.; Beauchamp, J.;  
418 Hansel, A.; Märk, T. D.; Weschler, C. J. Products of Ozone-Initiated Chemistry in a

- 419 Simulated Aircraft Environment. *Environ. Sci. Technol.* **2005**, *39*, 4823–4832.
- 420 (16) Wells, J. R.; Morrison, G. C.; Coleman, B. K. Kinetics and Reaction Products of Ozone  
421 and Surface-Bound Squalene. *J. ASTM Int.* **2008**, *5*, 101629.
- 422 (17) Jacobs, M. I.; Xu, B.; Kostko, O.; Heine, N.; Ahmed, M.; Wilson, K. R. Probing the  
423 Heterogeneous Ozonolysis of Squalene Nanoparticles by Photoemission. *J. Phys. Chem. A*  
424 **2016**, *120*, 8645–8656.
- 425 (18) Salvador, C. M.; Bekö, G.; Weschler, C. J.; Morrison, G.; Le Breton, M.; Hallquist, M.;  
426 Ekberg, L.; Langer, S. Indoor ozone/human chemistry and ventilation strategies. *Indoor*  
427 *Air* **2019**, *29*, 913–925.
- 428 (19) Anderson, S. E.; Franko, J.; Jackson, L. G.; Wells, J. R.; Ham, J. E.; Meade, B. J. Irritancy  
429 and Allergic Responses Induced by Exposure to the Indoor Air Chemical 4-Oxopentanal.  
430 *Toxicol. Sci.* **2012**, *127*, 371–381.
- 431 (20) Wolkoff, P.; Larsen, S. T.; Hammer, M.; Kofoed-Sørensen, V.; Clausen, P. A.; Nielsen,  
432 G. D. Human reference values for acute airway effects of five common ozone-initiated  
433 terpene reaction products in indoor air. *Toxicol. Lett.* **2013**, *216*, 54–64.
- 434 (21) Mochalski, P.; King, J.; Unterkofler, K.; Hinterhuber, H.; Amann, A. Emission rates of  
435 selected volatile organic compounds from skin of healthy volunteers. *J. Chromatogr. B.*  
436 **2014**, *959*, 62–70.
- 437 (22) Heine, N.; Houle, F. A.; Wilson, K. R. Connecting the Elementary Reaction Pathways of  
438 Criegee Intermediates to the Chemical Erosion of Squalene Interfaces during Ozonolysis.  
439 *Environ. Sci. Technol.* **2017**, *51*, 13740–13748.
- 440 (23) Heine, N.; Arata, C.; Goldstein, A. H.; Houle, F. A.; Wilson, K. R. Multiphase

- 441 Mechanism for the Production of Sulfuric Acid from SO<sub>2</sub> by Criegee Intermediates  
442 Formed during the Heterogeneous Reaction of Ozone with Squalene. *J. Phys. Chem. Lett.*  
443 **2018**, *9*, 3504–3510.
- 444 (24) Smith, J. D.; Kroll, J. H.; Cappa, C. D.; Che, D. L.; Liu, C. L.; Ahmed, M.; Leone, S. R.;  
445 Worsnop, D. R.; Wilson, K. R. The heterogeneous reaction of hydroxyl radicals with sub-  
446 micron squalane particles: a model system for understanding the oxidative aging of  
447 ambient aerosols. *Atmos. Chem. Phys* **2009**, *9*, 3209–3222.
- 448 (25) Zhao, J.; Zhang, R. Proton transfer reaction rate constants between hydronium ion (H<sub>3</sub>O<sup>+</sup>)  
449 and volatile organic compounds. *Atmos. Environ.* **2004**, *38*, 2177–2185.
- 450 (26) Kari, E.; Miettinen, P.; Yli-Pirilä, P.; Virtanen, A.; Faiola, C. L. PTR-ToF-MS product ion  
451 distributions and humidity-dependence of biogenic volatile organic compounds. *Int. J.*  
452 *Mass Spectrom.* **2018**, *430*, 87–97.
- 453 (27) Vlasenko, A.; MacDonald, A. M.; Sjostedt, S. J.; Abbatt, J. P. D. Formaldehyde  
454 measurements by proton transfer reaction - mass spectrometry (PTR-MS): correction for  
455 humidity effects. *Atmos. Meas. Tech.* **2010**, *3*, 1055–1062.
- 456 (28) Zhou, S.; Joudan, S.; Forbes, M. W.; Zhou, Z.; Abbatt, J. P. D. Reaction of Condensed-  
457 Phase Criegee Intermediates with Carboxylic Acids and Perfluoroalkyl Carboxylic Acids.  
458 *Environ. Sci. Technol. Lett.* **2019**, *6*, 243–250.
- 459 (29) Zhao, R.; Kenseth, C. M.; Huang, Y.; Dalleska, N. F.; Kuang, X. M.; Chen, J.; Paulson, S.  
460 E.; Seinfeld, J. H. Rapid Aqueous-Phase Hydrolysis of Ester Hydroperoxides Arising  
461 from Criegee Intermediates and Organic Acids. *J. Phys. Chem. A* **2018**, *122*, 5190–5201.
- 462 (30) Pagonis, D.; Sekimoto, K.; de Gouw, J. A Library of Proton-Transfer Reactions of H<sub>3</sub>O<sup>+</sup>

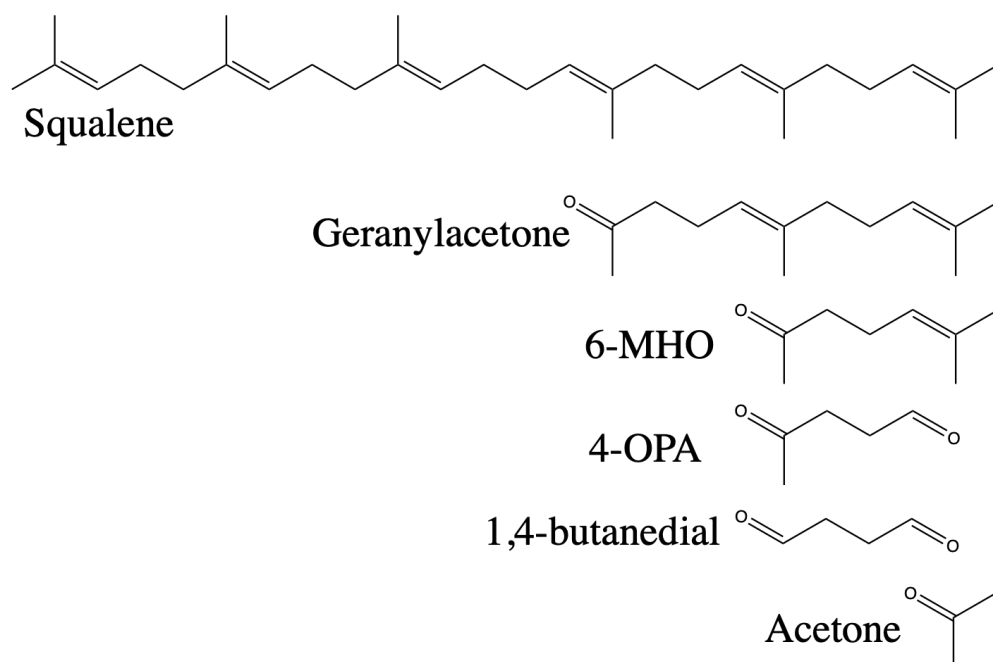
- 463 Ions Used for Trace Gas Detection. *J. Am. Soc. Mass Spectrom.* **2019**, *30*, 1330–1335.
- 464 (31) Petrick, L.; Dubowski, Y. Heterogeneous oxidation of squalene film by ozone under  
465 various indoor conditions. *Indoor Air* **2009**, *19*, 381–391.
- 466 (32) Fu, D.; Leng, C.; Kelley, J.; Zeng, G.; Zhang, Y.; Liu, Y. ATR-IR Study of Ozone  
467 Initiated Heterogeneous Oxidation of Squalene in an Indoor Environment. *Environ. Sci.*  
468 *Technol.* **2013**, *47*, 10611–10618.
- 469 (33) Wang, C.; Waring, M. S. Secondary organic aerosol formation initiated from reactions  
470 between ozone and surface-sorbed squalene. *Atmos. Environ.* **2014**, *84*, 222–229.
- 471 (34) Zhou, S.; Forbes, M. W.; Abbatt, J. P. D. Kinetics and Products from Heterogeneous  
472 Oxidation of Squalene with Ozone. *Environ. Sci. Technol.* **2016**, *50*, 11688–11697.
- 473 (35) Markowicz, P.; Larsson, L. Influence of relative humidity on VOC concentrations in  
474 indoor air. *Environ. Sci. Pollut. Res.* **2015**, *22*, 5772–5779.
- 475 (36) Andersen, I.; Lundqvist, G. R.; Mølhav, L. Indoor Air Pollution Due to Chipboard Used  
476 as a Construction Material. *Atmos. Environ.* **1975**, *9*, 1121–1127.
- 477 (37) Fang, L.; Clausen, G.; Fanger, P. O. Impact of temperature and humidity on chemical and  
478 sensory emissions from building materials. *Indoor Air* **1999**, *9*, 193–201.
- 479 (38) Huang, H.; Haghghat, F.; Blondeau, P. Volatile organic compound (VOC) adsorption on  
480 material: influence of gas phase concentration, relative humidity and VOC type. *Indoor*  
481 *Air* **2006**, *16*, 236–247.
- 482 (39) Huang, S.; Xiong, J.; Cai, C.; Xu, W.; Zhang, Y. Influence of humidity on the initial  
483 emittable concentration of formaldehyde and hexaldehyde in building materials:  
484 experimental observation and correlation. *Sci. Rep.* **2016**, *6*, 23388.

- 485 (40) Liang, W.; Yang, S.; Yang, X. Long-Term Formaldehyde Emissions from Medium-  
486 Density Fiberboard in a Full-Scale Experimental Room: Emission Characteristics and the  
487 Effects of Temperature and Humidity. *Environ. Sci. Technol.* **2015**, *49*, 10349–10356.
- 488 (41) Parthasarathy, S.; Maddalena, R. L.; Russell, M. L.; Apte, M. G. Effect of Temperature  
489 and Humidity on Formaldehyde Emissions in Temporary Housing Units. *J. Air Waste*  
490 *Manag. Assoc.* **2011**, *61*, 689–695.
- 491 (42) Sidheswaran, M.; Chen, W.; Chang, A.; Miller, R.; Cohn, S.; Sullivan, D.; Fisk, W. J.;  
492 Kumagai, K.; Destailats, H. Formaldehyde Emissions from Ventilation Filters under  
493 Different Relative Humidity Conditions. *Environ. Sci. Technol.* **2013**, *47*, 5336–5343.
- 494 (43) Xu, J.; Zhang, J. S. An experimental study of relative humidity effect on VOCs' effective  
495 diffusion coefficient and partition coefficient in a porous medium. *Build. Environ.* **2011**,  
496 *46*, 1785–1796.
- 497 (44) Won, D.; Corsi, R. L.; Rynes, M. Sorptive interactions between VOCs and indoor  
498 materials. *Indoor Air* **2001**, *11*, 246–256.
- 499 (45) Shen, J.; Gao, Z. Ozone removal on building material surface: A literature review. *Build.*  
500 *Environ.* **2018**, *134*, 205–217.
- 501 (46) Gall, E.; Darling, E.; Siegel, J. A.; Morrison, G. C.; Corsi, R. L. Evaluation of three  
502 common green building materials for ozone removal, and primary and secondary  
503 emissions of aldehydes. *Atmos. Environ.* **2013**, *77*, 910–918.
- 504 (47) Anderson SE, Franko J, Jackson LG, Wells J, Ham JE, Meade B. Irritancy and allergic  
505 responses induced by exposure to the indoor air chemical 4-oxopentanal. *Toxicol Sci.*  
506 **2012**, *127*, 371–381.

507

508

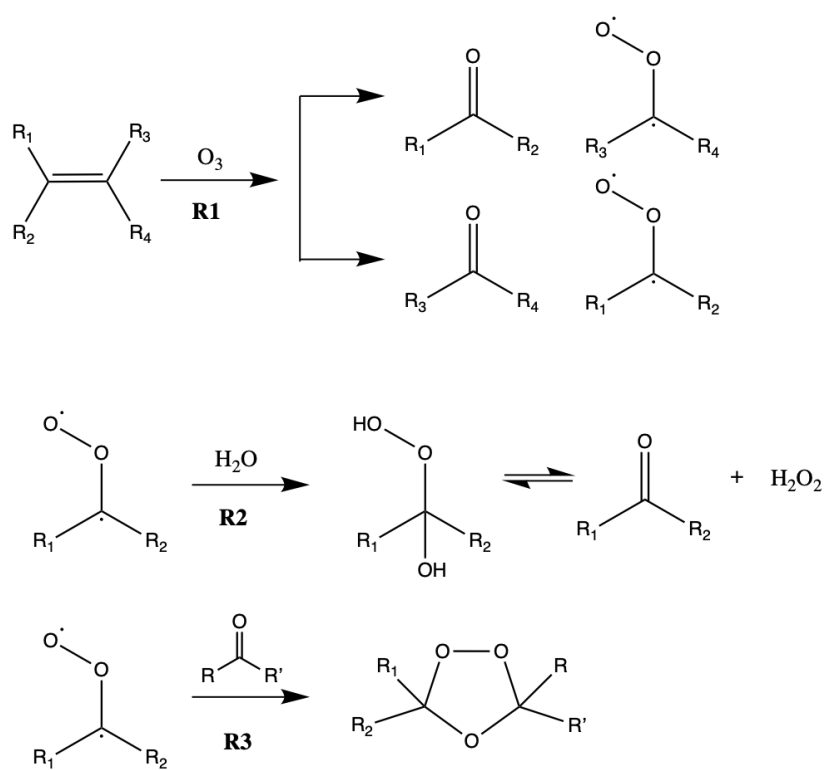
509



**Figure 1:** Chemical structure of squalene and selected squalene ozonolysis products



## Scheme 1: Simplified Reaction Mechanism for Ozonolysis of Alkenes



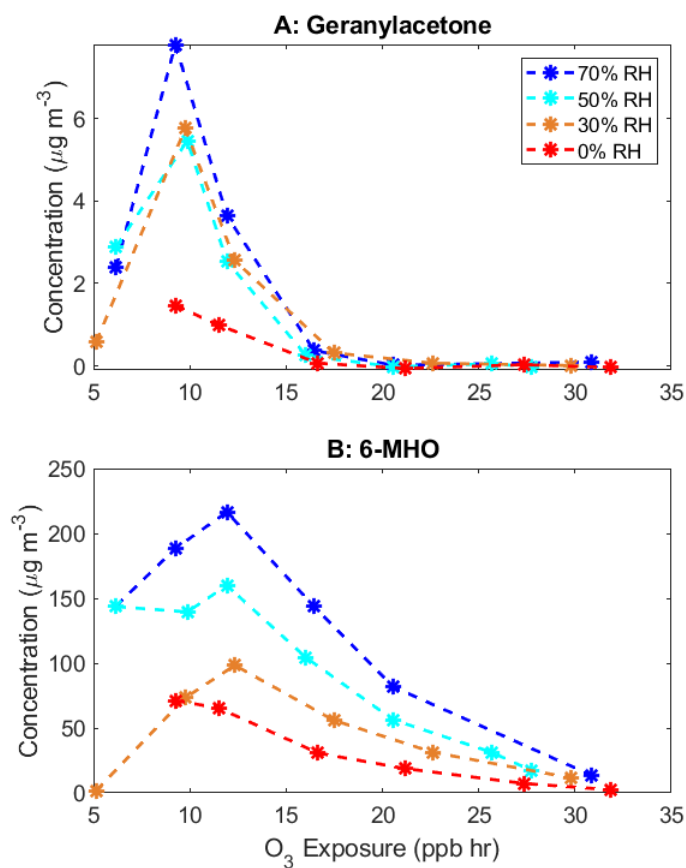


**Figure 2:** Primary unsaturated products from squalene ozonolysis as a function of humidity and O<sub>3</sub> exposure.

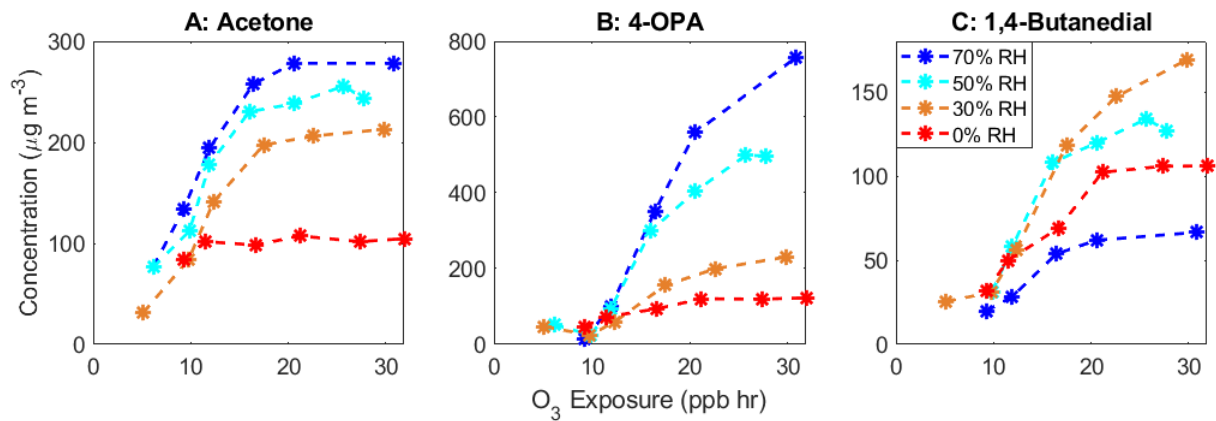


**Figure 3:** Terminal products from squalene ozonolysis as a function of humidity and  $O_3$  exposure.

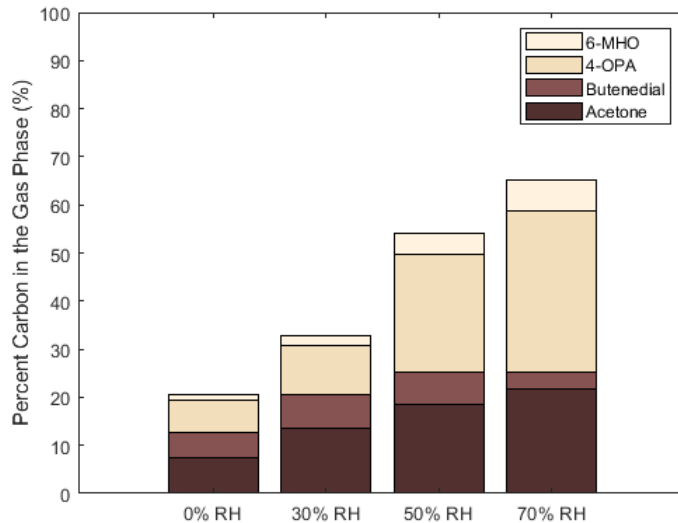


**Figure 4:** Percent of carbon in the gas phase at 20 ppb h  $O_3$  exposure as a function of RH. Converting the measurements in Figures 2-3 from  $\mu g m^{-3}$  to  $\mu g C m^{-3}$ , and normalizing to the initial concentration of carbon entering the flow tube gives the percent carbon in the gas phase.

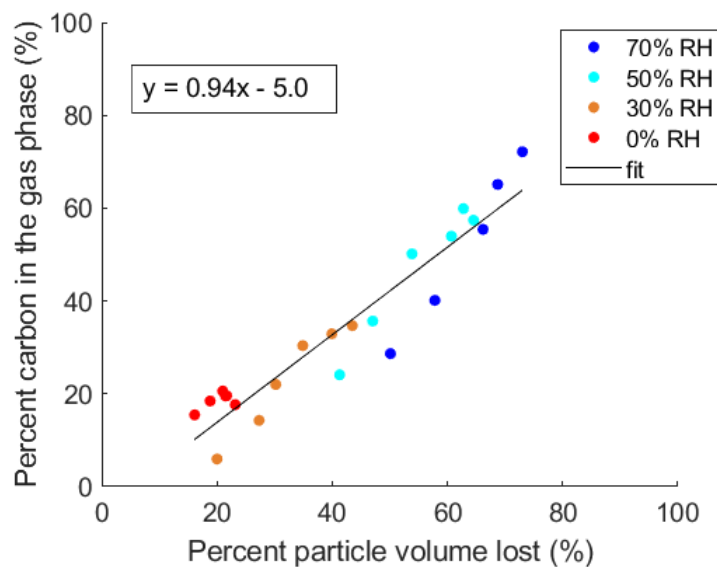


**Figure 5:** Percent carbon in the gas phase compared to the percent of particle volume lost for all RH and  $O_3$  exposures.

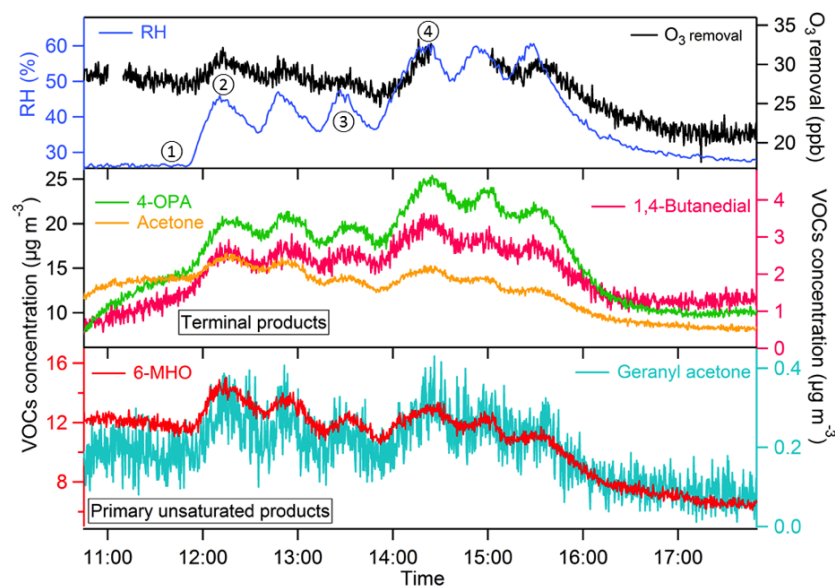


**Figure 6:** Time series of primary unsaturated products (lower panel) and terminal products (middle panel) with relative humidity and O<sub>3</sub> removal (upper panel) for clothing experiment (O<sub>3</sub> removal was obtained by subtracting measured O<sub>3</sub> level from the level of O<sub>3</sub> in supply air; the gap in the O<sub>3</sub> removal curve is due to the measurement of O<sub>3</sub> level in supply air). Circled numbers in the top panel refer to conditions referenced in Table 1.

**Table 1:** The concentration change of squalene oxidation products ( $\Delta\text{VOCs}$ ,  $\mu\text{g m}^{-3}$ ) due to relative humidity (RH) increase. Circled numbers refer to points in Figure 6.

RH (%)	$\Delta\text{O}_3$ (ppb)	$\Delta\text{VOCs}$ ( $\mu\text{g m}^{-3}$ )							
		acetone	4-OPA	6-MHO	geranyl acetone	1,4- butanediol	hydroxy acetone	4-oxobutanoic acid	5-hydroxy-4- oxopentanal
① 26	② 2.90	2.17	5.91	2.54	0.117	1.14	1.28	0.340	0.339
44									
③ 46	④ 3.37	0.960	5.09	0.652	0.084	0.812	0.881	0.327	0.284
59									